The catalytic activity of Pt_nCu_m (n+m=3, m≠3) clusters for methanol dehydrogenation to CO

Qingyun Wang (w_qingyun@163.com)
Hexi University
Chun-Yan Wang
Hexi University
Yong-Chun Tong
Hexi University
Xin-Jian Xu
Hexi University
Qing-Ling Bai
Hexi University
Shou-Bo Li
Hexi University

Research Article

Keywords: Density functional theory, Methanol, PtCu catalyst

Posted Date: March 22nd, 2021

DOI: https://doi.org/10.21203/rs.3.rs-315716/v1

Abstract

Based on the density functional theory (DFT), the geometric for the reactants, intermediates, transition states and dehydrogenation products have been optimized. The energy diagrams are drawn out along both the O-adsorption path and H-adsorption path, and the C-H bond scission pathway is energetically more favorable than the O-H bond scission pathway. By calculation, the Pt is the active site in the whole reaction processes, and the barrier energy of the rate-determining step is 11.09 kcal/mol by Pt: Cu=2: 1 which is lower than that of Pt 3 and PtCu 2 . Importantly, it is shown that the complete dehydrogenation product of methanol, CO, can more easily dissociate from PtCu 2 cluster than from Pt 3 cluster. Therefore, Cu doping can promote the catalytic activity of Pt in a certain extent.

Introduction

At present, PtCu binary metal catalyst has attracted great attention of scientists due to its good oxidation activity, stability and anti-poisoning performance for methanol of direct methanol fuel cells (DMFCs), and many research groups have achieved excellent results [1-14]. Chen et al. [10] have found that hollow PtCu octahedral nanoalloys are efficient bifunctional electrocatalysts towards oxygen reduction reaction and methanol oxidation reaction by regulating near-surface composition. Baronia group [6] has revealed that the electro-catalytic activity of the synthesized PtCu/N-rGO catalyst is much higher to that of Pt/N-rGO and Pt/C catalyst by cyclic voltammetry, electrochemical impedance spectroscopy and electron transfer measurements. The maximum activity per unit mass of $Pt_{32}Cu_{68}$ NWs prepared by Liao et al. [11] is two times higher than that of Pt nanowires, and it shows very high stability and tolerance to CO poisoning. The enhanced activity and stability are attributed to the bifunctional mechanism. It is considered that the alloy copper atoms in Pt lattice provide common manipulation sites to reduce the poisoning effect of CO intermediate species on NWs active surface sites. The optimal alloy ratio of PtCu nanoparticles prepared by Khan et al. [12] is 20 *wt*%, and the activity per unit mass is 0.043 *m*A/*μg*Pt. The results show that the electronic structure of Pt in PtCu alloy is modified due to the shift of *d*-band center of Pt, which can reduce CO poisoning and improve the catalytic activity of methanol oxidation and oxygen reduction reaction. Wei et al [14] have reported by theoretical research that the catalyst of Pt_3Cu_4 cluster has good catalytic effect for methanol decomposition and it is selective toward CO_2 over CO. In this paper, we choose Pt_nCu_m (n+m=3, m≠3) clusters as catalysts to study the dehydrogenation behavior of methanol on PtCu alloy.

The study on the mechanism of methanol electro-oxidation over Pt-based catalysts is helpful for us to understand the catalytic activity of anode Pt-based catalyst in DMFCs, and to design and develop high-efficiency catalyst based on bifunctional mechanism and ligand (electron) effect. To develop DMFCs and provide comprehensive mechanistic insights, a large number of studies have been devoted to understand the methanol oxidation reaction processes on Pt electrodes. Two possible reaction paths for dehydrogenation of methanol to CO are proposed, one is methyl-adsorption (H-adsorption) initiated C-H

bond cleavage [15-17], and the other is oxygen-adsorption (O-adsorption) initiated O-H bond cleavage [17-22].

In this paper, we have studied the catalytic mechanism of methanol over Pt_nCu_m (n+m=3, m≠3) by density functional theory (DFT), and found that when the ratio of platinum and copper is different, the catalytic performance is quite different.

Computational Details And Models

In the present study, the calculations have been performed using the Gaussian 09 code [23]. As for the optimized structures and vibration frequencies of all the stationary points, density functional theory (DFT) with hybrid B3LYP functional is employed [24-26]. In order to include the Van der Waals interaction between the catalyst and methanol, Grimme's dispersion correction (DFT-D3 (BJ)) is applied [27, 28]. The Los Alamos LANL2DZ effective core pseudopotentials (ECP) is employed for Pt and Cu, while the C, H and O atoms are treated with 6-311++G(d, p) basis set [29, 30]. During geometrical optimizations, symmetric constraints are not imposed, and the optimized minima and transition states are confirmed by vibration frequency calculations. Intrinsic reaction coordinates (IRC) calculations [31] are used to connect reactants and products, and the zero points energy (ZPE) corrections are performed at the same level.

It is generally believed that gas-phase clusters can be used as a model system to illustrate the complex catalytic mechanisms in the realistic nano-catalytic reaction [32, 33]. The simplest Pt_3, Pt_2Cu and $PtCu_2$ clusters to simulate the catalytic mechanism of methanol dehydrogenation reaction. Considering that the ground states of the three clusters are singlet states, we calculated the methanol dehydrogenation over Pt_3, Pt_2Cu and $PtCu_2$ clusters on the singlet potential energy surface.

Results And Discussion

In this paper, the mechanism of methanol dehydrogenation reaction initiated by O-adsorption and H-adsorption over Pt_3, Pt_2Cu and $PtCu_2$ clusters are described, respectively. The dehydrogenation path of methanol initiated by O-adsorption on Pt_nCu_m (n+m=3, m≠3) cluster (O-adsorption path) is divided into four continuous dehydrogenation steps: $CH_3OH \rightarrow CH_3O \rightarrow CH_2O \rightarrow CHO \rightarrow CO$. There are three possible dehydrogenation pathways initiating by H-adsorption (H-adsorption path): (1) $CH_3OH \rightarrow CH_2OH \rightarrow CH_2O \rightarrow CHO \rightarrow CO$; (2) $CH_3OH \rightarrow CH_2OH \rightarrow CHOH \rightarrow CHO \rightarrow CO$; (3) $CH_3OH \rightarrow CH_2OH \rightarrow CHOH \rightarrow COH \rightarrow CO$.

By comparing the reactions of CH_3OH+ Pt_nCu_m (n+m=3, m≠3), it is explained the reasons why PtCu binary metal nanomaterials show superior catalytic activity for methanol oxidation.

CH_3OH+Pt_3

In Fig. 1 and Fig. 2, methanol is adsorbed on the top of Pt atom by O atom, and the adsorption energy is 17.45kcal/mol, which is very close to the calculation result of Pang (-16.87 kcal/ mol) [16]. Compared with the free methanol molecule, the O-H bond is slightly elongated, which indicates that the O-H bond of methanol is not activated well. Therefore, the energy barrier of a1→a2 is very high by 24.90kcal/mol, which indicate that the dehydrogenation of hydroxyl group is difficult in kinetics. The energy barrier of the next three dehydrogenation reactions is much lower than that of the first step of O-H bond breaking. Therefore, the first step of O-H bond breaking is the speed-determining step of the whole path, which is consistent with Kandoi's [34] conclusion. Finally, in the product complex a5, four H atoms in methanol have been transferred to Pt3 cluster, and the product1 and CO are formed by Pt-C bond breaking with the dissociated energy of 30.26 kcal/mol. It shows that the dissociation of CO is very difficult, which is also the reason why Pt catalyzes methanol reaction is easy to be poisoned.

In Fig. 3 and 4, the intermediated a6 is initial adsorption configuration with the adsorption energy of -6.62 kcal/mol, which is lower than that of a1. Karp et al [35] experimentally determined that the adsorption energy of methanol on Pt(111) surface at 100K is -14.5±0.2 kcal /mol. Once a6 is formed, the C-H bond activated by Pt is easy to break, that is, only the transition state of a6-7 with the energy barrier of 3.56 kcal/mol needs to be flipped to form the intermediate a7, which is close to the energy barrier of 4.84 kcal/mol calculated by Hartnig et al. [15]. The O-H bond of intermediated a7 is broken through the transition state of a7-8. In this process, the distance of O-H bond is obviously elongated. It should be noted that this step is completed by the interaction of two Pt atoms with the barrier of the reaction of 8.05kcal/mol. With the break of the second and third C-H bonds, the final product complex a10 is formed, which has mirror symmetry with a5. The energy barriers of these two steps are 12.89kcal/mol and 11.69kcal/mol, respectively. For H-adsorption path, the energy of intermediates and transition states in path (1) are below the reactants, and the reaction energy barrier of the whole dehydrogenation process is very low, which is the most likely to occur in the three paths. For path (2) and (3), the energy barriers are 26.95kcal/mol and 48.54kcal/mol, respectively, so path (2) and (3) is difficult to compete with path (1). Compared with H-adsorption and O-adsorption path, path (1) initiated in H-adsorption path is most likely to occur.

In the process of methanol dehydrogenation, Pt catalyst makes the O-H bond and C-H bond of methanol to stretch continuously and activated until breaks. The intermediates CH_3O, CH_2O, CHO and the dehydrogenation product CO in the pathway have good adsorption stability, which lead to Pt catalyst poisoning. It can be seen from Fig. 1 and 3, the activation of O-H and C-H bond in methanol mainly occurs one Pt atom, which indicates that the catalytic behavior of small Pt cluster is different from that on Pt crystal plane, and the catalytic reaction of methanol on Pt crystal plane involves the interaction of 2-4 adjacent Pt atoms [35]. Neurock et al. considered that the clusters composed of 1-4 Pt atoms all play an important role in the electro-catalytic oxidation of methanol, and single Pt atom, Pt dimer and Pt trimer supported on graphene are observed under scanning tunneling microscope [36].

CH_3OH+Pt_2Cu

The dehydrogenation of methanol initiated by O-adsorption on Pt_2Cu cluster can be divided into two types: O-adsorption occurs at Pt site and Cu site respectively. By calculation, the adsorption energy of O atom at Cu site is 1.51kcal/mol lower than that at Pt site. Although there is a strong interaction between O and Cu, the hydroxyl hydrogen gradually approaches Pt, resulting in O-H bond breaking and formation of Pt-H bond. The next dehydrogenation reaction takes place at Pt sites. The energy barrier of this step ($CH_3OH \rightarrow CH_3O$) is the highest in the whole path, which is the speed-determining step with the energy barrier of 51.09 kcal /mol. Such a high energy barrier makes the reaction almost impossible, which is nearly two times higher than that of Pt_3 (24.90 kcal / mol). At the same time, we also calculated the energy barrier of O-H bond breaking at Pt site (32.89 kcal /mol), which is higher than that of Pt_3. It shows that the addition of Cu has little effect on the O-adsorption path.

The adsorption energy of H-adsorption on Pt site is 2.82 kcal/mol lower than that at Cu site, which indicates that methyl hydrogen is more likely to attack Pt site in Pt_2Cu. Fig. 5 depicts the geometries of all transition states and intermediates in the dehydrogenation reaction initiated by H-adsorption on Pt_2Cu cluster. The potential energy surface profile of the reaction path is given in Fig. 6. In path (1), the methyl hydrogen in methanol attacks the Pt site of Pt_2Cu cluster to form the initial reaction complex b6. Then, starting from b6, the first C-H bond is broken through a lower energy barrier to form a stable intermediate b7 (Fig. 5 and 6). b7 is a very important intermediate for the H-adsorption path, and the subsequent dehydrogenation reactions start from b7. For the next O-H bond breaking (b7→b7-8→b8) of path (1), the hydroxyl hydrogen in methanol gradually approaches to another Pt atom, resulting in O-H cleavage, and the energy barrier of this step is 11.09 kcal / mol. After the transition states of b8-9 and b9-10, the next two C-H bonds are broken, and the corresponding energy barriers are 9.44 kcal/mol and 10.38kcal/mol, respectively, in which Cu participates in the second C-H bond breaking process (Fig. 5). The energy barrier of the whole dehydrogenation process is low. The synergistic effect of Cu leads to the dehydrogenation reaction more easily. In the final product compound b10, the dissociation energy of dissociating CO from b10 is 31.37 kcal/mol, which is similar to that of dissociating CO from a10 (30.27 kcal/mol).

In Fig. 6, the relatively high energy barrier of O-H bond breaking (28.64kcal/mol) is the rate-determining step of path (2), and the energy barrier of rate-determining step of path (3) is 35.72kcal/mol, which is higher that of path (2) and (1) . Therefore, it is difficult for path (2) and path (3) to compete with path (1). In addition to CO, Pt_2Cu has good poison resistance to other carbon-containing intermediates.

$CH_3OH+PtCu_2$

The reaction pathway of methanol dehydrogenation initiated by O-adsorption on $PtCu_2$ cluster is similar to that of Pt_2Cu. The oxygen atom of methanol is more easily to adsorb on the Cu site, and the corresponding adsorption energy is 4.65kcal/mol, which is lower than that of Pt site. By calculation, the energy barrier of O-H bond breaking of methanol at Cu and Pt site are 47.14kcal/mol and 42.88 kcal /mol, respectively, which is the rate-determining step of the O-adsorption path. The addition of Cu is not conducive to the first O-adsorption path.

The same as the calculation result of the reaction between methanol and Pt_2Cu, methyl hydrogen in methanol is more likely to attack Pt sites in $PtCu_2$. In Fig. 7 and 8, the adsorption energy of c6 (4.84 kcal/mol) is higher than that of b6 and a6. For path (1) and (2) of H-adsorption path, the breaking of O-H bond becomes the rate-determining step of these paths, and the corresponding energy barrier is 29.41kcal/mol and 29.14kcal/mol, respectively. Therefore, path (1) and path (2) of H-adsorption path are two competing reactions. The rate-determining step of path (3) is the third C-H bond breaking, and the corresponding energy barrier is 50.68kcal/mol. Such a high energy barrier means that this path is difficult to react. This is mainly because the CHOH structure in c11 is stable, making the C-H bond difficult to break. Liao and Baronia et al reported [6, 11] that when Pt:Cu=1:2, the catalytic activity is significantly improved. For $PtCu_2$, although the dehydrogenation energy barrier of methanol is slightly higher than that of Pt_2Cu and Pt_3, it is significantly easier to remove CO and reactivate the Pt sites of the catalyst. This may be one of the reasons for the higher catalytic activity of $PtCu_2$ than pure Pt.

Comparative analysis

The rate-determining step of O-adsorption path on Pt_3, Pt_2Cu and $PtCu_2$ clusters is the first dehydrogenation reaction, that is, the breaking process of O-H bond. The difficulty of dehydrogenation prevents the subsequent reaction from taking place, which indicates that Cu doping has little effect on O-adsorption path.

In path (1) of H-adsorption path, the energy barrier of methanol dehydrogenation over Pt_2Cu is 1.8kcal/mol lower than that on Pt_3. For the Pt sites of H-adsorption path, both adsorption and dehydrogenation are easier, which indicates that doping Cu in Pt catalyst can improve the catalytic activity of the catalyst and reduce the cost of the catalyst. As for a6, b6 and c6, the stability of b6 is higher than that of a6, while that of c6 is lower than that of a6. The change law of adsorption energy is consistent with the intrinsic activity law of the catalyst, that is, Pt_2Cu has the highest catalytic activity. The rate-determining step of path (3) occurs in the third C-H bond breaking process, i.e. CHOH→COH. Compared with the other two paths, the energy barrier of this path is highest. In Fig. 4, 6 and 8, the structures of a11, b11 and c11 are similar, and the C-O bond ($r_{C\text{-}O}$=1.3 Å) is shorter than that of methanol, which shows that the interaction between CHOH is strengthened and the C-H bond is difficult to break. $PtCu_2$ has better resistance to CO poisoning, which maybe the reason why it has better catalytic activity than pure Pt. The results are consistent with the experimental results of Li et al [37].

As shown in Fig. 9, although Pt has both the ability to accept and donate electrons, Pt has a stronger ability to accept electrons. Therefore, the lone pair of electrons on O atom in methanol is easier to transfer to the *d*-orbital of Pt in the catalyst, that is, the electrons transfer from the HOMO of methanol to the LUMO of the catalyst, resulting in a stronger interaction. Thus, the O-adsorption stability of methanol on the Pt_nCu_m (n+m=3, m≠3) clusters is stronger than that of H-adsorption. In Pt_2Cu, Cu atom has a positive charge of +0.390e and Pt atom has a negative charge of -0.195e. The O atom of methanol is more easily adsorbed on the Cu site due the negative charge, while the methyl hydrogen is more likely to be adsorbed

on the Pt site because of its positive charge. Because of Cu doping, the interaction between methyl hydrogen and Pt_2Cu is stronger than that of Pt_3. For $PtCu_2$, when methyl hydrogen interacts with Pt, because Pt has more negative charges, the repelling ability between Pt and O in methanol is also the largest, which makes the whole methanol molecule far away from Pt, resulting in the decrease of H-adsorption ability. From the frontier molecular orbital, there is almost no interaction between methanol and $PtCu_2$. As shown in Fig. 9, the matching of LUMO of Pt_2Cu and $PtCu_2$ with HOMO of methanol is not as good as that of Pt_3, which is also the reason why the adsorption stability of O-adsorption of the two catalysts is not as good as that of Pt_3.

It should be noted that the salvation effect of the system is ignored in our calculations. However, the generally accepted view is that the salvation effect is expected to have similar effects on the three clusters, so that he main conclusions we get in the gas phase calculations are valid [32]. A study of the reactions of free clusters can provide useful information for understanding the mechanisms involved in the realistic and complicated catalytic systems.

Conclusions

In this paper, we have performed a comparative theoretical study the dehydrogenation process of methanol on Pt_nCu_m (n+m=3, m≠3) clusters. The conclusions are as follow:

(1) By comparing the dehydrogenation of methanol on Pt_nCu_m (n+m=3, m≠3) clusters, the whole process from methanol dehydrogenation to CO is exothermic.

(2) The rate-determining step of O-adsorption path on Cu and Pt sites of Pt_nCu_m (n+m=3, m≠3) clusters is the first step, i.e. the breaking of O-H bond. Cu doping did not promote the O-adsorption path.

(3) There are three dehydrogenation pathways of H-adsorption path on Pt site of Pt_nCu_m (n+m=3, m≠3) clusters. For Pt_3 and Pt_2Cu clusters, the optimal pathway is path (1), and for $PtCu_2$, path (1) and path (2) are competitive. Although the energy barrier of the rate-determining step of H-adsorption path on $PtCu_2$ is higher than that on Pt_3 and Pt_2Cu, $PtCu_2$ catalyst is more beneficial to improve the anti-CO poisoning performance.

(4) Difference electrons carried by Pt and Cu sites in binary metal alloys lead to different adsorption sites. Compared with each reaction path, Cu doping can promote the catalytic activity of Pt in a certain extent.

Declarations

Funding This article was funded by the Natural Science Foundation of Gansu (No.20JR5RA199), National Natural Science Foundation (No.21865007), and Special Project of Hexi University (No. HXZX10).

Data availability The datasets generated during and/or analyzed during the current study are available from the corresponding author on reasonable request.

Authors' contributions All authors contributed to the study conception and design. Material preparation and data collection were performed by Chun-Yan Wang, Yong-Chun Tong, Xin-Jian Xu, Qing-Ling Bai and Shou-Bo Li. Data analysis was performed by Qing-Yun Wang. The first draft of the manuscript was written by Qing-Yun Wang and all authors commented on previous versions of the manuscript. All authors read and approved the final manuscript.

Code availability N/A.

Declarations

Ethics approval N/A.

Consent to participate N/A.

Consent for publication N/A.

Conflict of interest The authors declare no competing interests.

References

1. Huang L, Zhang W, Zhong Y, et al. (2020) Surface-structure tailoring of ultrafine PtCu nanowires for enhanced electrooxidation of alcohols. Science China-Materials, 64: 601-610.
2. Ye S H, He X J, Ding L X, et al. (2020) Cu_2O template synthesis of high-performance PtCu alloy yolk-shell cube catalysts for direct methanolfuel cells (vol 50, pg 12337, 2014). Chemical Communications, 56: 1114-11142.
3. Song T S, Xue H, Guo N K, et al. (2020) Dual-modulation of electronic structure and active sites of PtCu nanodendrites by surface nitridation to achieve efficient methanol electrooxidation and oxygen reduction reaction. Chemical Communications, 56: 7136-7139.
4. Xiang H, Zheng Y, Sun Y, et al. (2020) Bimetallic and postsynthetically alloyed PtCu nanostructures with tunable reactivity for the methanoloxidation reaction. Nanoscale Advances, 2: 1603-1612.
5. Peng X, Chen D, Yag X, et al. (2016) Microwave-assisted synthesis of highly dispersed PtCu nanoparticles on three-dimensional nitrogen-doped graphene networks with remarkably enhanced methanol electrooxidation. ACS Applied Materials & Interfaces, 8: 33673-33680.
6. Baronia R, Goel J, Gautam G, et al. (2019) Synthesis and characterization of nitrogen doped reduced graphene oxide (N-rGO) supported PtCu anode catalysts for direct methanol fuel cell. Journal of Nanoscience and Nanotechnology, 19: 3832-3843.
7. Cao J, Du Y, Dong M, et al. (2018) Template-free synthesis of chain-like PtCu nanowires and their superior performance for oxygen reduction and methanol oxidation reaction. Journal of Alloys and Compounds, 747: 124-130.
8. Lu L, Chen S, Thota S, et al. (2017) Composition controllable synthesis of PtCu nanodendrites with efficient electrocatalytic activity for methanol oxidation induced by high index surface and electronic

interaction. Journal of Physical Chemistry C, 121: 19796-19806.

9. Pavlets A S, Alekseenko A A, Tabachkova N Yu, et al. (2021) A novel strategy for the synthesis of Pt-Cu uneven nanoparticles as an efficient electrocatalyst toward oxygen reduction. International Journal of Hydrogen Energy, 46: 5355-5368.
10. Chen G, Yang X, Xie Z, et al. (2020) Hollow PtCu octahedral nanoalloys: Efficient bifunctional electrocatalysts towards oxygen reduction reaction and methanol oxidation reaction by regulating near-surface composition. Journal of Colloid and Interface Science, 562: 244-251.
11. Liao Y, Yu G, Zhang Y, et al. (2016) Composition-tunable PtCu alloy nanowires and electrocatalytic synergy for methanol oxidation reaction. Journal of Physical Chemistry C, 120: 10476-10484.
12. Khan I A, Qian Y, Badshah A, et al. (2016) Fabrication of highly stable and efficient PtCu alloy nanoparticles on highly porous carbon for direct methanol fuel cells. ACS Applied Materials &Interfaces, 8: 20793-20801.
13. Sun J, Shi J, Xu J, et al. (2015) Enhanced methanol electro-oxidation and oxygen reduction reaction performance of ultrafine nanoporous platinum-copper alloy: Experiment and density functional theory calculation. Journal of Power Sources, 279: 334-344.
14. Wei A, Feng W, Liu H, et al. (2017) Methanol activation catalyzed by Pt7, Pt3Cu4, and Cu7 clusters: A density functional theory investigation. Applied Organometallic Chemistry, 32: e4197.
15. Hartnig C, Spohr E. (2005) The role of water in the initial steps of methanol oxidation on Pt(111). Chemical Physics, 319: 185-191.
16. Pang S K. (2015) Why palladium cathodes can bear resistance to methanol but not platinum cathodes. Electrochimica Acta, 161: 420-426.
17. Zhang W, Liu Y, Zhang D, (2012) A comparative theoretical study for the methanol dehydrogenation to CO over Pt_3 and $PtAu_2$ clusters. J Mol Model, 18: 3051-3060
18. Watanabe T, Ehara M, Kuramoto K, et al. (2009) Possible reaction pathway in methanol dehydrogenation on Pt and Ag surfaces/clusters starting from O–H scission: Dipped adcluster model study. Surf. Sci. 603: 641-646.
19. Sheng T, Lin X, Chen Z, et al. (2015) Methanol electro-oxidation on platinum modified tungsten carbides in direct methanol fuel cells: a DFT study, Surf. Sci. 2015, 17: 25235-25243.
20. Greeley J, Mavrikakis M. (2004) Competitive Paths for Methanol Decomposition on Pt(111). J. Am. Chem. Soc. 126: 3910-3919.
21. Greeley J, Mavrikakis M. (2002) A First-Principles Study of Methanol Decomposition on Pt(111). J. Am. Chem. Soc. 124: 7193-7201.
22. Valentin D, Fittipaldi D, Pacchioni G. (2015) Methanol oxidation reaction on α-tungsten carbide versus platinum (111) surfaces: a DFT electrochemical study. ChemCatChem,7: 3533-3543.
23. Frisch M J, Trucks G W, Schlegel H B, et al. Gaussian 09, Revision A.02, Gaussian Inc., Wallingford, CT 2009.

24. Becke A D. (1993) Density-functional thermochemistry. III. Therole of exact exchange. J Chem. Phys., 98:5648-5652.
25. Becke A D. (1988) Density-functional exchange-energy approximation with correct asymptotic behavior. Phys Rev A, 38: 3098-3100.
26. Lee C T, Yang W T, Parr R G. (1988) Development of the Colic-Salvetti correlation-energy formula into a functional of the electron density. Phys Rev B 37: 785-789.
27. Grimme S, Ehrlich S, Goerigk L. (2011) Effect of the damping function in dispersion corrected density functional theory. J. Comput. Chem. 32: 1456.
28. Grimme S, Antony J, Ehrlich S, et al. (2010) A consistent and accurate ab initio parametrization of density functional dispersion correction (DFT-D) for the 94 elements H-Pu. J. Chem. Phys. 132: 154104.
29. Hay P J, Wadt W R. (1985) Ab initio effective core potentials for molecular calculations. Potentials for the transition metal atoms Sc to Hg. J Chem Phys 82: 270-283.
30. Hay P J, Wadt W R (1985) Ab initio effective core potentials for molecular calculations. Potentials for K to Au including the outermost core orbitals. J Chem Phys 82: 299-310.
31. Fukui K (1970) A formulation of the reaction coordinate, J Phys Chem 74: 4161-4163.
32. Fialko E F, Kikhtenko A V, Goncharov V B, et al. (1997) Similarities between reactions of methanol with $Mo_xO_y^+$ in the gas phase and over real catalysts. J Phys Chem B 101: 5772-5773.
33. Wallace W T, Whetten R L (2002) Coadsorption of CO and O_2 on selected gold clusters: Evidence for efficient room-temperature CO_2 generation. J Am Chem Soc 124: 7499-7505.
34. Kandoi S, Greeley J, (2006) Sanchez-Castillo M A, et al. Prediction of experimental methanol decomposition rates on platinum from first principles. Topics in Catalysis, 37: 17-28.
35. Karp E M, Silbaugh T L, Crowe M C, et al. (2012) Energetics of adsorbed methanol and methoxy on Pt (111) by microcalorimetry. Journal of the American Chemical Society, 134: 20388-20395.
36. Neurock M, Janik M, Wieckowski A. (2009) A first principles comparison of the mechanism and site requirements for the electrocatalytic oxidation of methanol and formic acid over Pt. Faraday Discuss, 140: 363-378.
37. Li H H, Fu Q Q, Xu L, et al. (2017) Highly crystalline PtCu nanotubes with three dimensional molecular accessible and restructured surface for efficient catalysis. Energy & Environmental Science, 10: 1751-1756.

Figures

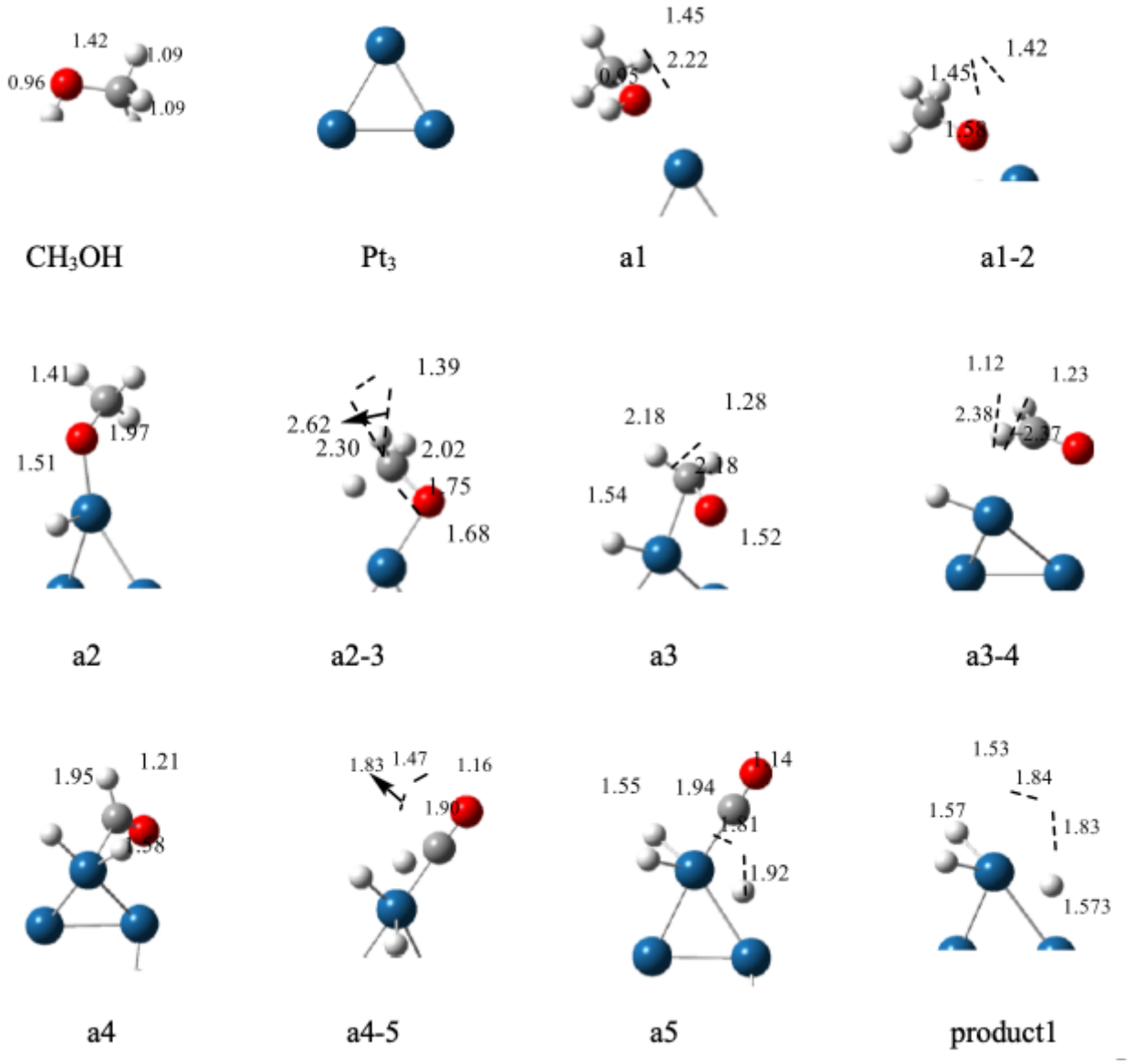

Figure 1

The intermediates and transition states optimized in the dehydrogenation of O-adsorption path on Pt3 (The blue, gray, red and white spheres represent Pt,C,H and O atoms, respectively. The unit of length is Å, the same as below)

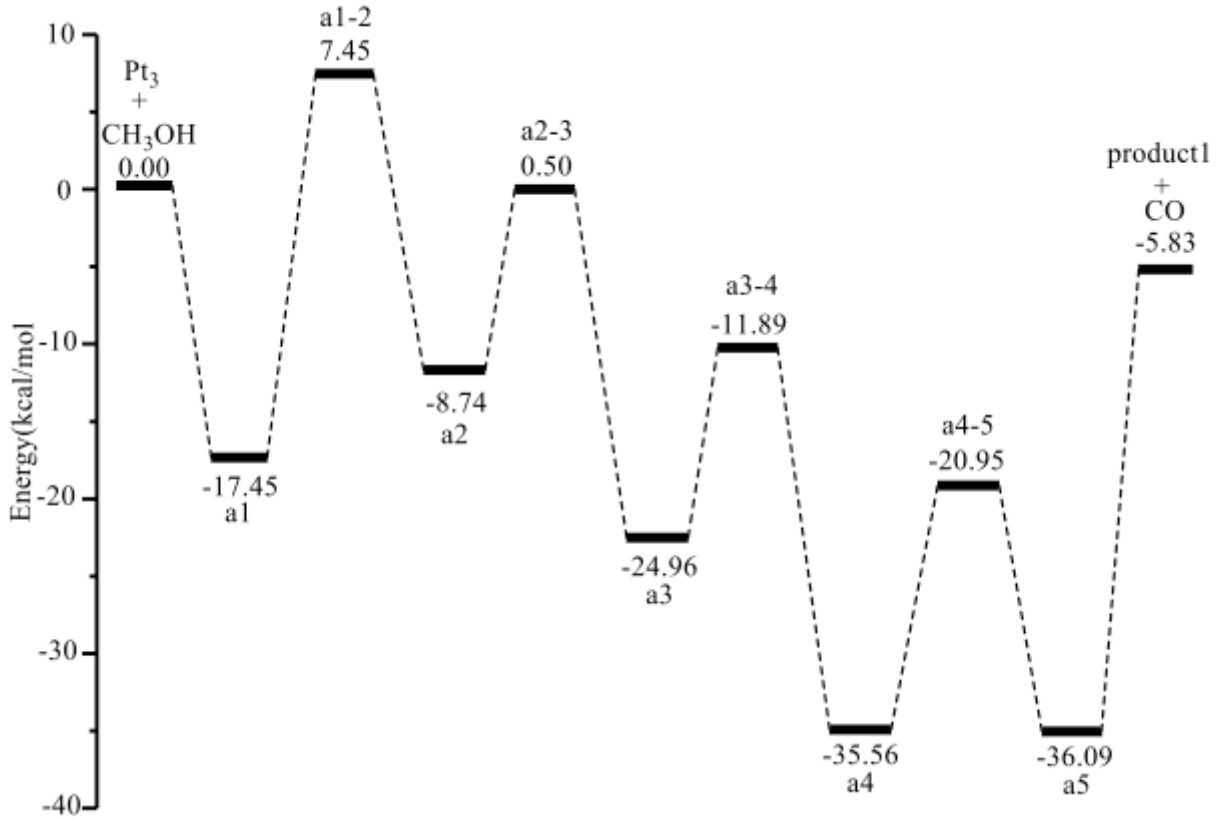

Figure 2

The potential energy profile of O-adsorption path on Pt3

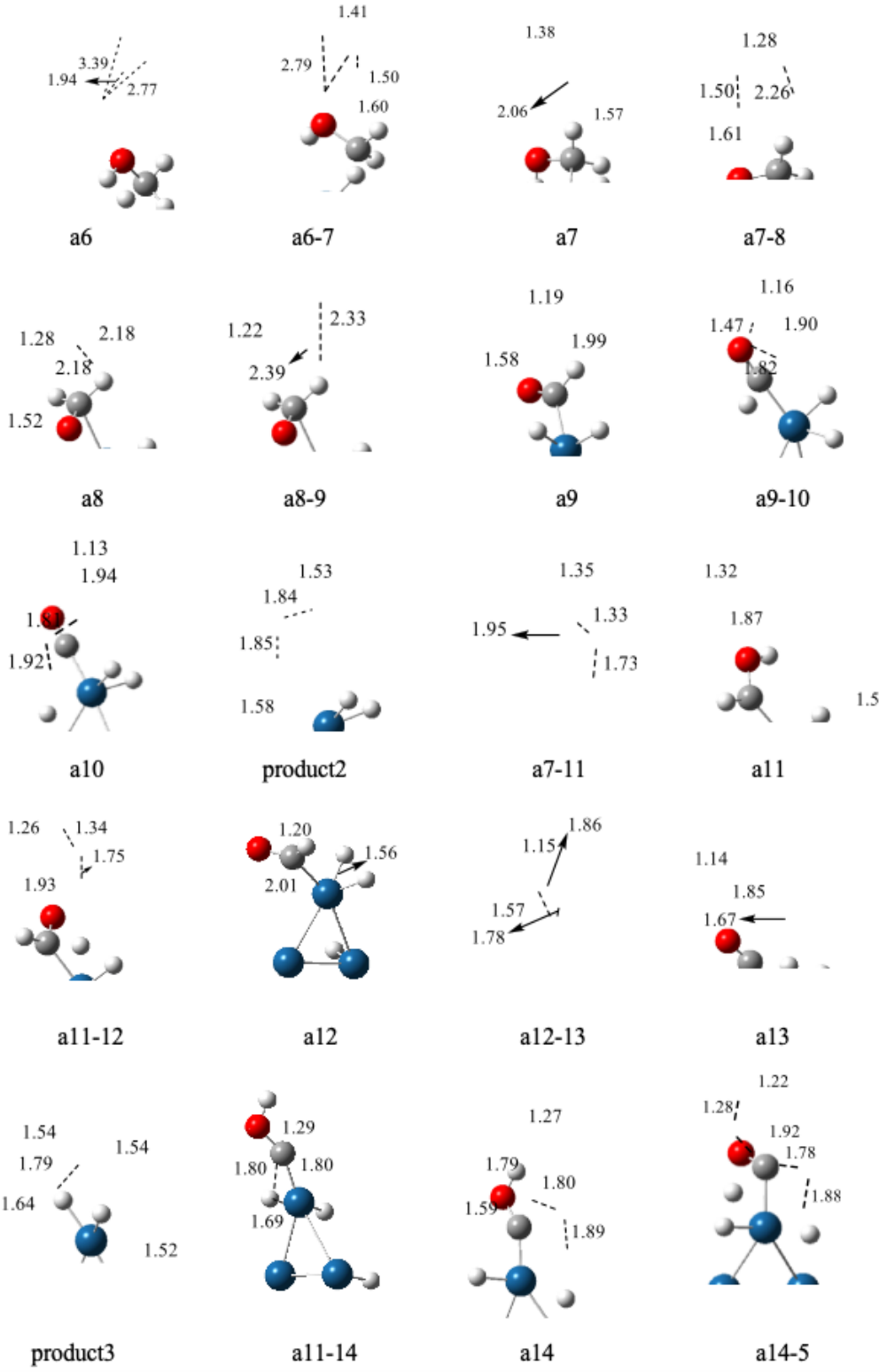

Figure 3

The intermediates and transition states optimized in the dehydrogenation of H-adsorption path on Pt3

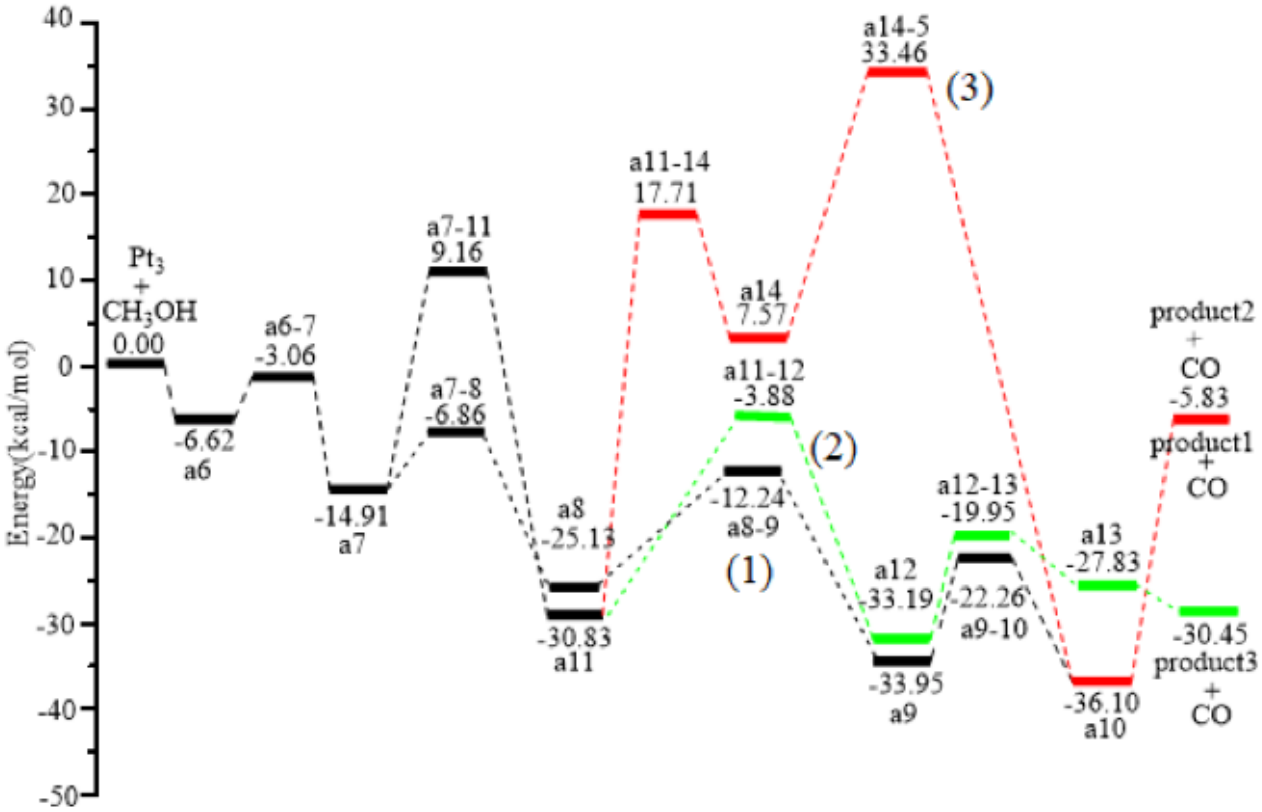

Figure 4

The potential energy profile of H-adsorption path on Pt3

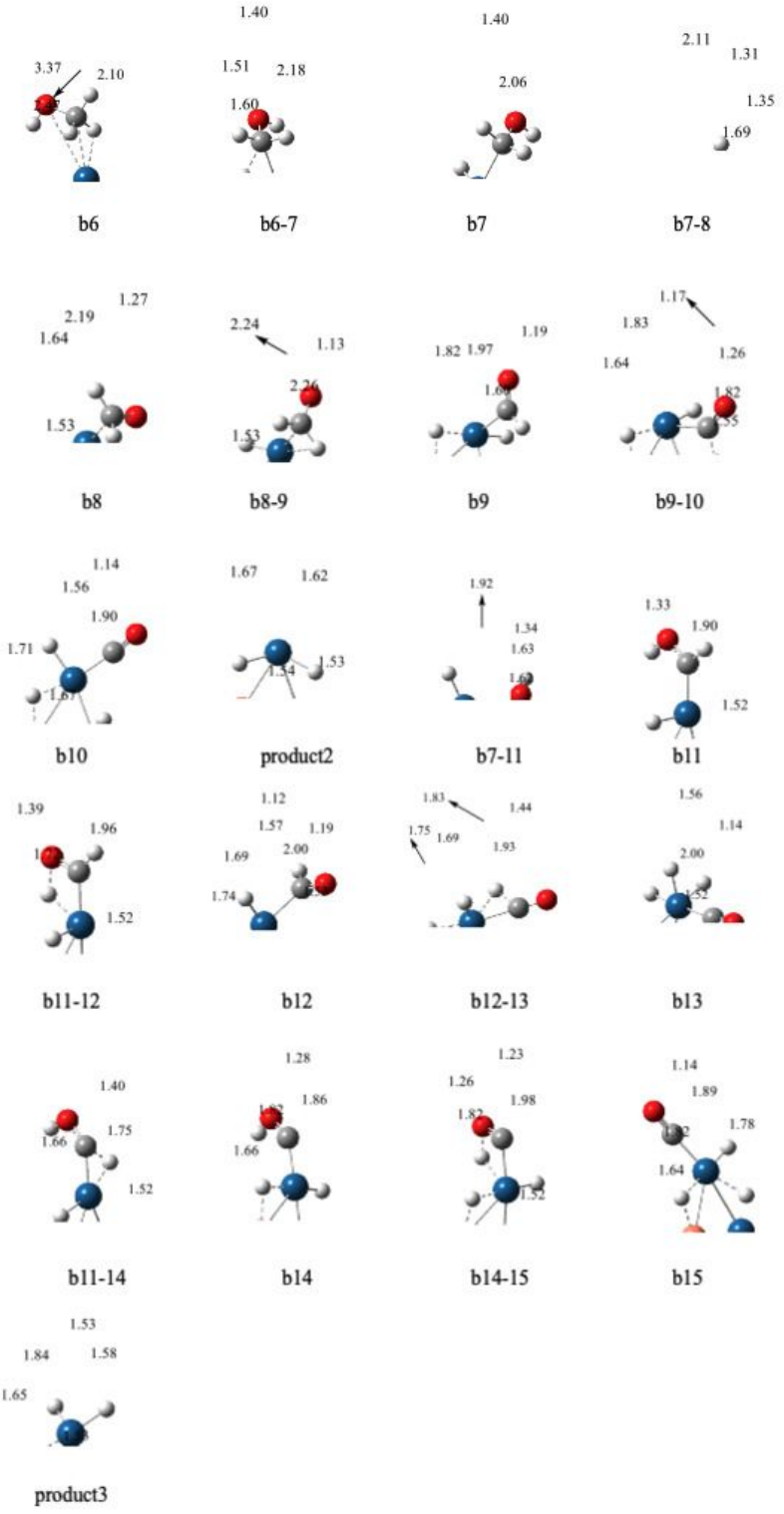

Figure 5

The intermediates and transition states optimized in the dehydrogenation of H-adsorption path on Pt2Cu

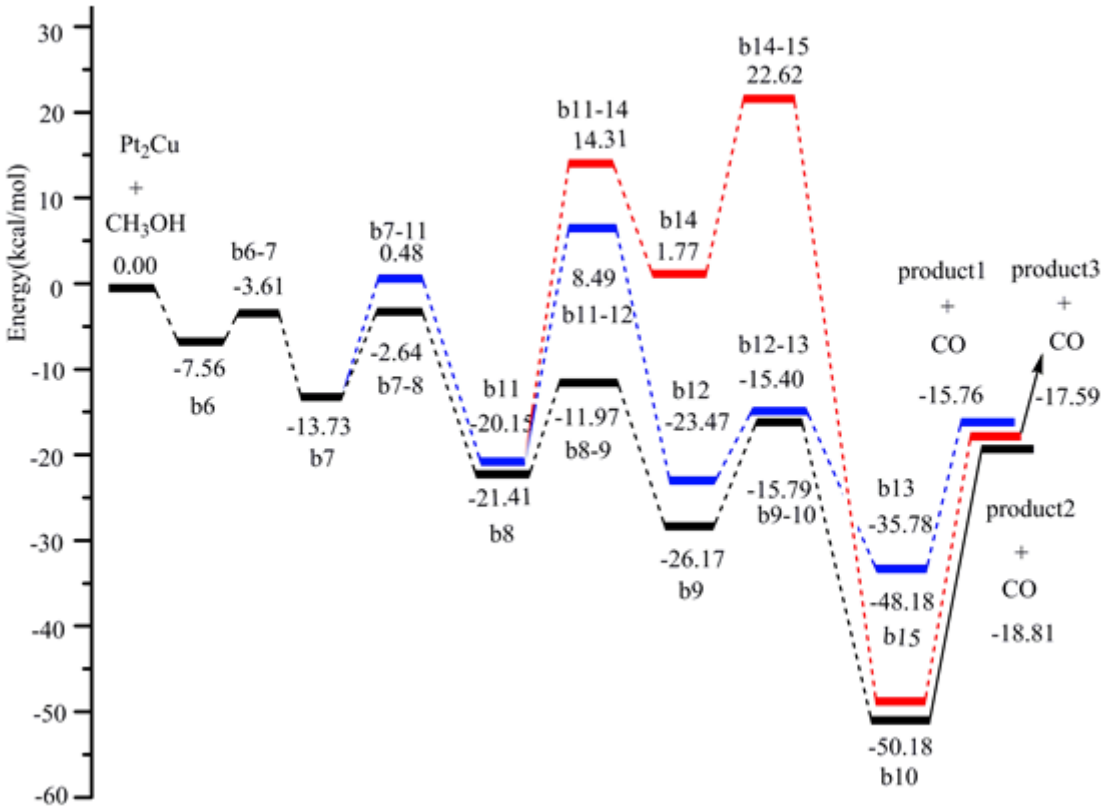

Figure 6

The potential energy profile of H-adsorption path on Pt2Cu

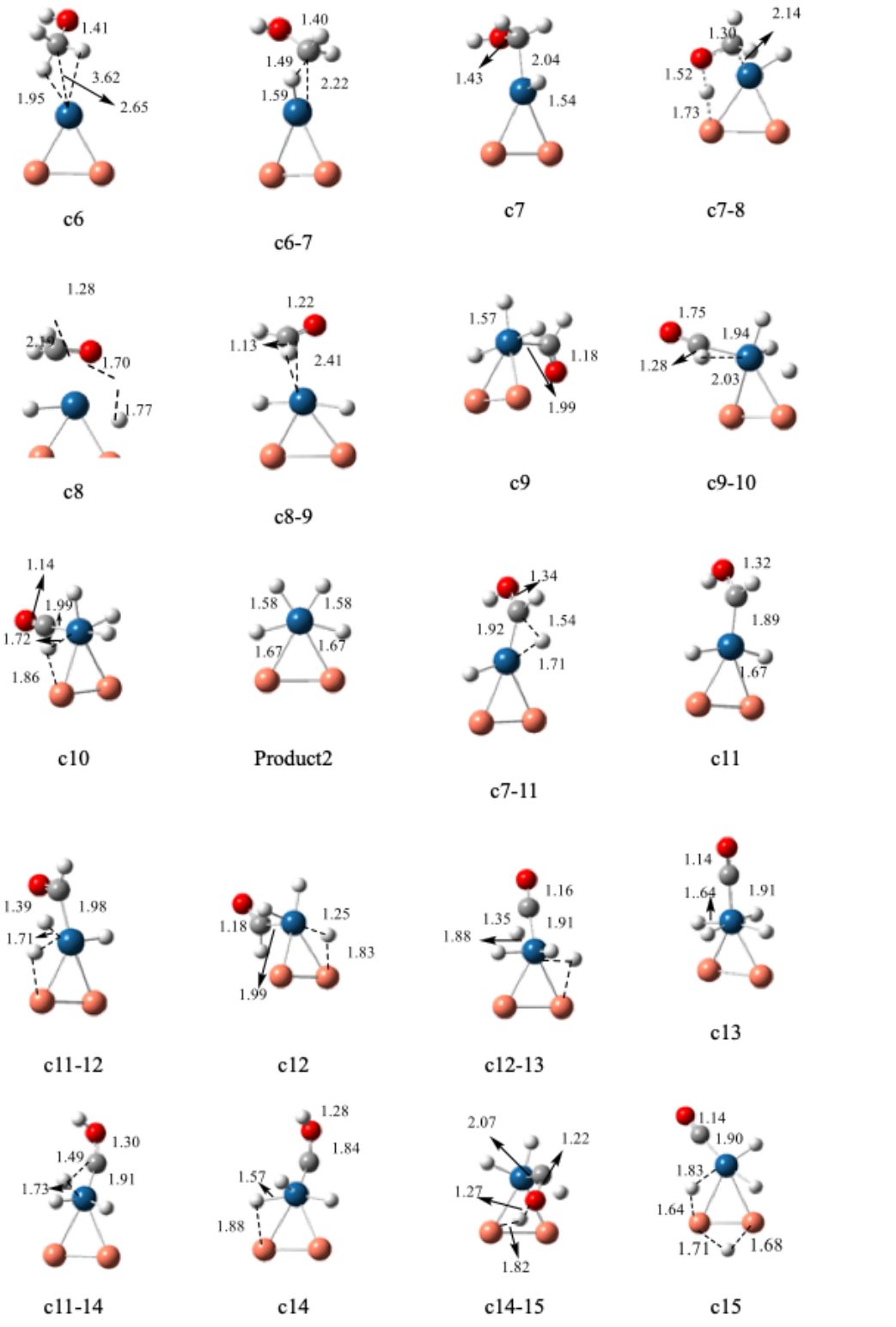

Figure 7

The intermediates and transition states optimized in the dehydrogenation of H-adsorption path on PtCu2

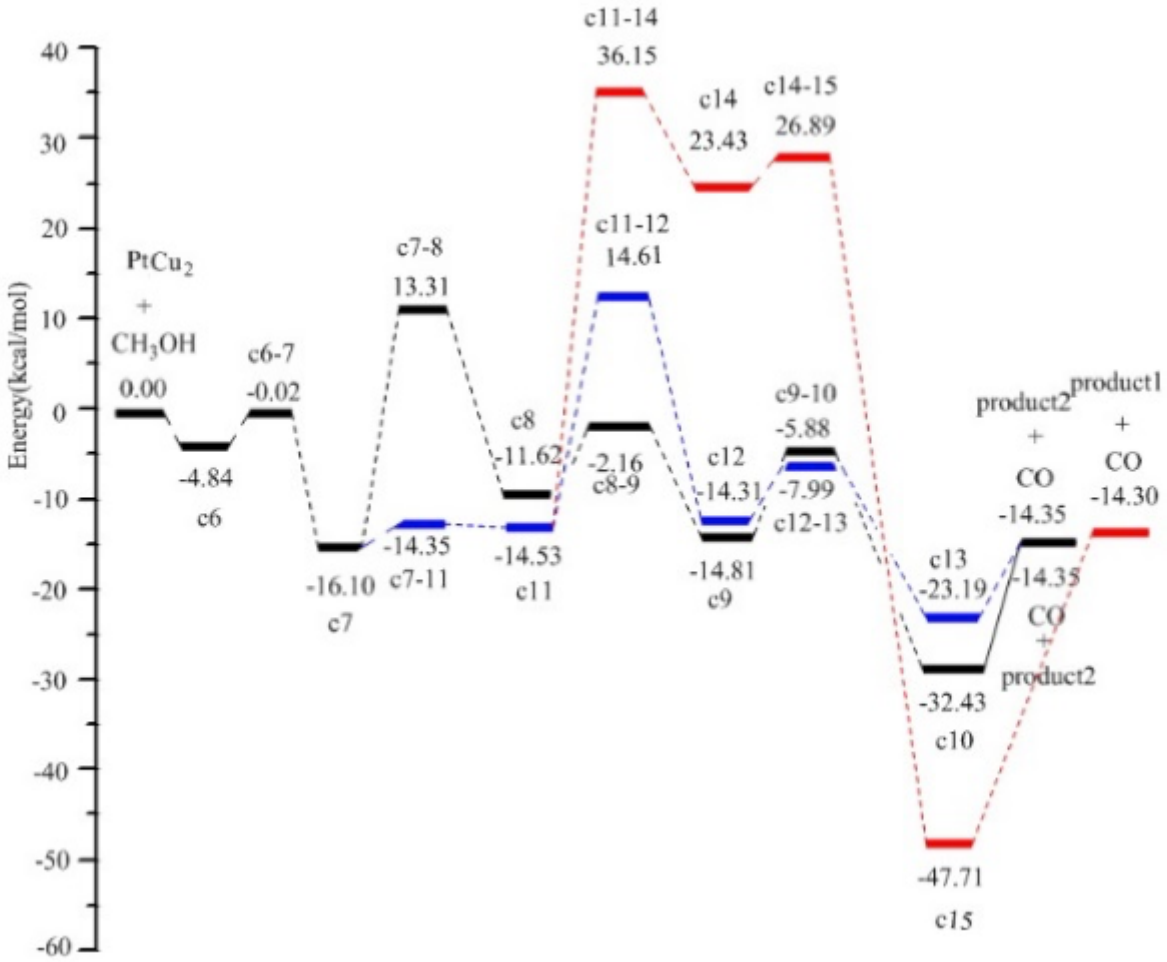

Figure 8

The potential energy profile of H-adsorption path on PtCu2

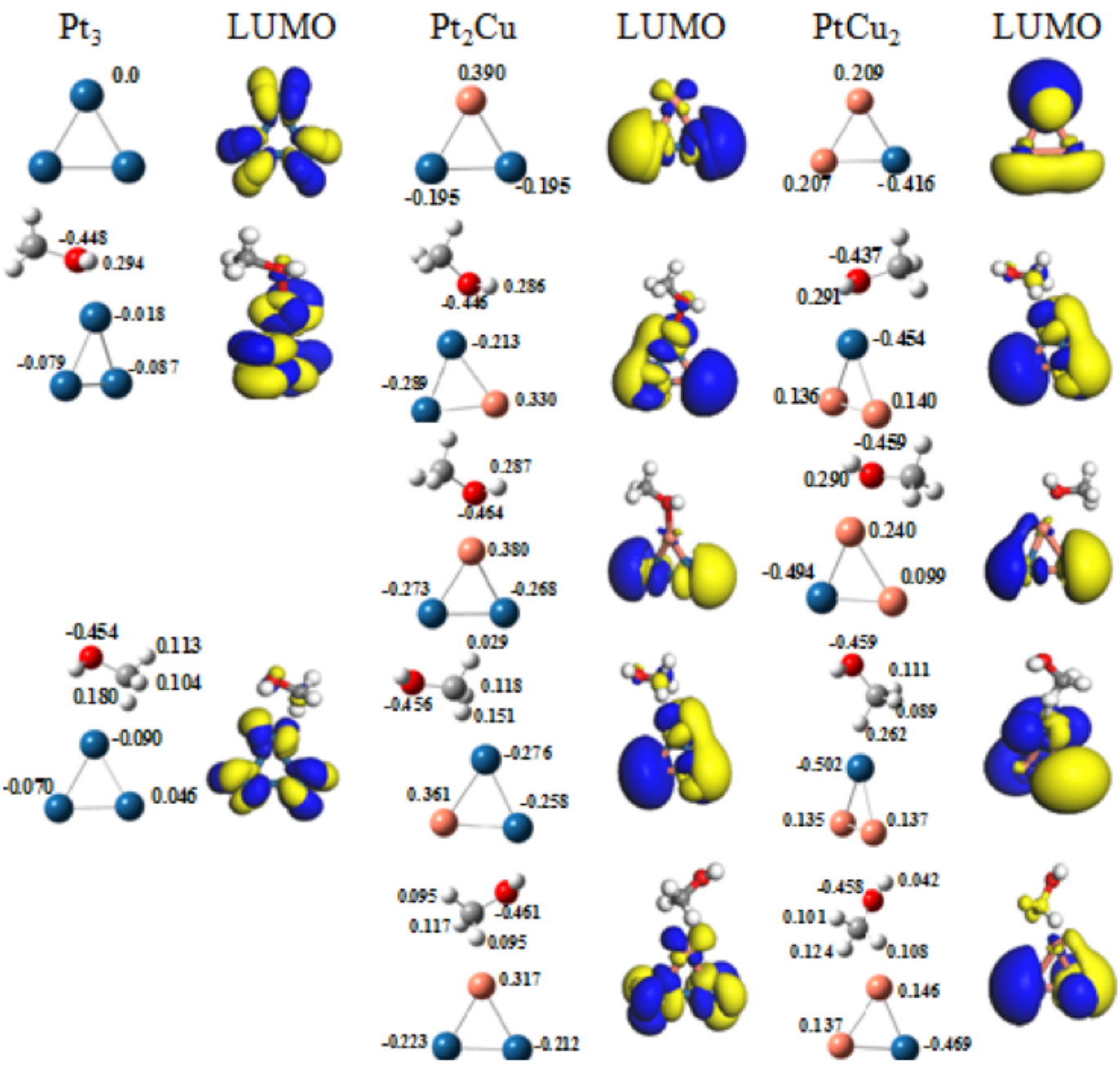

Figure 9

The NBO charge and frontline molecular orbital diagram before and after methanol adsorption by Pt3, Pt2Cu and PtCu2